CRPP

Suprathermal Electron Studies in the TCV Tokamak: Design of a Tomographic Hard-X-Ray Spectrometer

ÉCOLE POLYTECHNIQUE FÉDÉRALE DE LAUSANNE

S. Gnesin[1], S. Coda[1], J. Decker[2], Y. Peysson[2]

[1]École Polytechnique Fédérale de Lausanne (EPFL), Centre de Recherches en Physique des Plasmas (CRPP)
Association Euratom - Confédération Suisse, CH-1015 Lausanne, Switzerland

[2]Association Euratom-CEA, CCEA/DSM/IRFM, CEA Cadarache,
13108 St Paul lez Durance, France

Introduction and motivations

Electron cyclotron resonance heating (ECRH) and current drive (ECCD)[1], disruptive events, and sawtooth activity[2] are all known to produce suprathermal electrons in fusion devices, motivating increasingly detailed studies of the generation and dynamics of this suprathermal population. Measurements have been performed in past years in the TCV tokamak[3] using a single pinhole hard-X-ray (HXR)[4,5] camera and electron-cyclotron-emission (ECE)[6] radiometers, leading in particular to the identification of the crucial role of spatial transport in the physics of ECCD[7] . The observation of a poloidal asymmetry in the emitted suprathermal bremsstrahlung radiation motivates the design of a proposed new tomographic HXR spectrometer, reported in this poster. The design, which is based on a compact, modified Soller collimator concept, is being aided by simulations of tomographic reconstruction. Quantitative criteria have been developed to optimize the design for the greatly variable shapes and positions of TCV plasmas.

Suprathermal electron generation in TCV

Electron energy distribution function

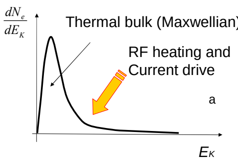

Radio frequency (RF) waves (~GHz) transfer energy to electrons by resonant interaction.

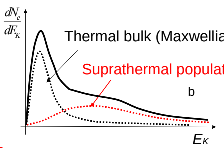

➤ Electron cyclotron resonance heating (ECRH) and current drive (ECCD)

2nd harmonic (X-mode) :
6 steerable launchers
Power: 0.5 MW each
Frequency: 82.7 GHz
Density limit: 4X10^{19} m^{-3}
Pulse length: 2s

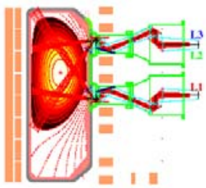

3rd harmonic (X-mode) :
1 upper steerable launcher
Power: 1.5 MW
Frequency: 118 GHz
Density limit: 1.1X10^{20} m^{-3}
Pulse length: 2s

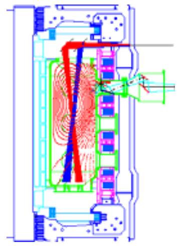

➤ Disruptive instability events and magnetic reconnection:

Neoclassical Tearing Modes (NTM)
Sawtooth activity [8]

Review of TCV Results

RF field-particle resonance interaction (ECRH; ECCD)

Suprathermal electron population is generated

➤**Bremsstrahlung emission (hard X-rays)** due to electron-ion collisions.

➤**ECE emission** due to the Larmor motion predominantly from suprathermals on HFS or obliquely on LFS.

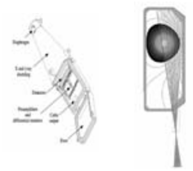

The HXR camera on loan from TORE SUPRA[4,5] clearly evidenced the LFS-HFS asymmetry of the poloidal bremsstrahlung distribution (possibly related to trapped particles)

Other diagnostics used:
- ➤ high-field-side electron cyclotron emission (ECE) radiometer [6]
- ➤ oblique ECE [9]
- ➤multiwire proportional chamber [10]
- ➤ diamagnetic loop coil

New diagnostics being installed:
- •tangential HXR camera
- •vertical ECE

X2 generates suprathermal electrons and contributes to enhance the X3 power absorption [11]

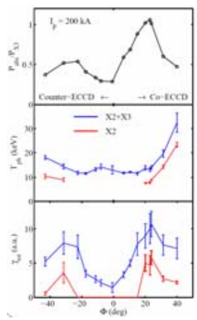

Fast electron broadening from transport observed in many ECCD discharges (resulting in ECCD profile broadening) [7]

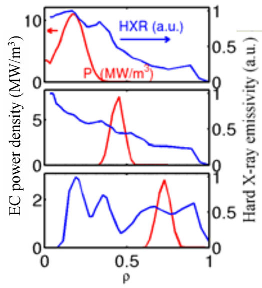

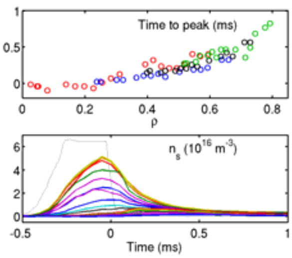

Suprathermal density propagation in space after short ECCD pulses measured by HFS ECE and coherently averaged [12].
The time at which the ECE signal peaks at a given radial position (time to peak) is affected by the characteristic radial diffusion time of the suprathermal electron population.

Proposed tomographic spectroscopic system for TCV

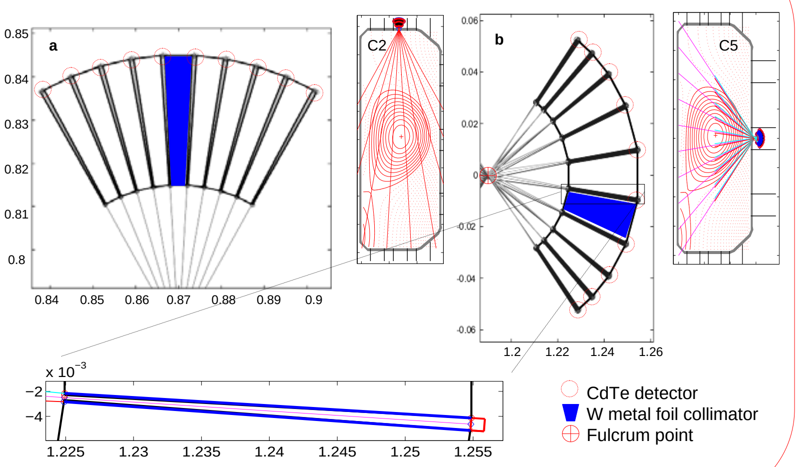

➤ **Design for up to nine spectroscopic HXR cameras [C1,…,C9] on the right figure.**

➤ **Novel collimator system design adapted from the Soller collimator concept [13]: radially-disposed Soller plates.**

Two limiting concepts can be envisioned:
a) Uniform angular detector spacing: provides finer spatial resolution near the instrument axis than at its edges. suitable for cameras with a small fan aperture as in the case of mainly vertically viewing cameras (C1, C2, C3, C7, C8, C9 but also C4 and C6).
b) Uniform chord separation on any plane perpendicular to the camera axis. advantageous in the case of camera C5, which has a wider angular fan view.

- ➤ Radial detector array (~30 CdTe detectors)
- ➤ Modified Soller Collimator design : tungsten metal foil with adjustable collimator aperture:
  - control the photon statistics
  - guarantee oblique photon shielding
- ➤ Filters (Al, S.S.) and vacuum windows (Be)
- ➤ Wide poloidal coverage
- ➤ Adaptable to other fusion devices

- ➤ Time resolution: down to 1 ms
- ➤ Energy resolution: ~ 5keV at 60keV of photon energy
- ➤ Pile up limit: ~1MHz
- ➤ Energy range: 20-200 keV
- ➤ Spatial sampling: ~ 2 cm

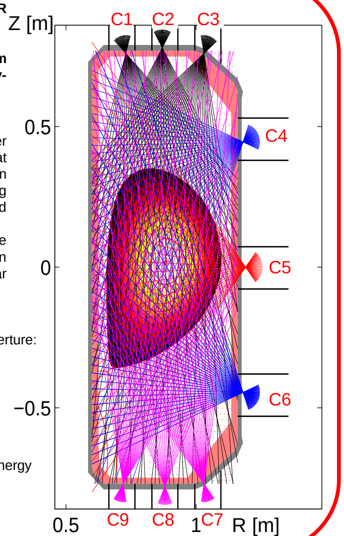

17th Topical Conference on High-Temperature Plasma Diagnostics, May 11-15 2008, Albuquerque, NM, USA

CRPP

ÉCOLE POLYTECHNIQUE FÉDÉRALE DE LAUSANNE

Suprathermal Electron Studies in the TCV Tokamak: Design of a Tomographic Hard-X-Ray Spectrometer

Tomographic reconstruction procedure

Tomographic reconstruction of a 2D emission pattern on the TCV poloidal plane

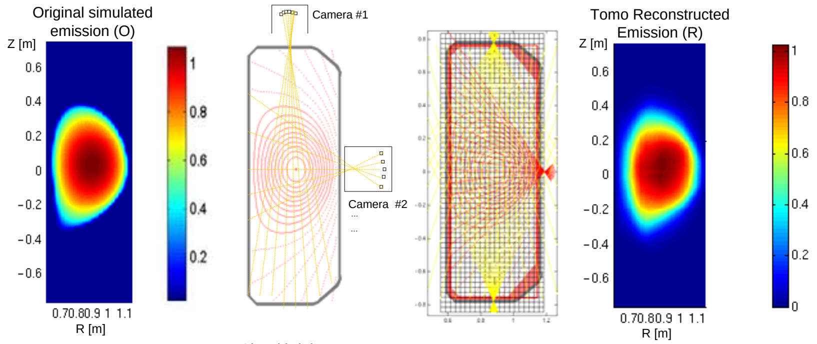

Simulated Original 2D Emission *g(R,z)*

Chord brightness $f_i = \int g(R,z)\, dL$

Tomographic emission reconstruction on a pixel grid. *f=T*g*

g is obtained using a Minimum Fisher information method

Minimum Fisher information regularization [14,15]

$$f_i = T_{i,p} \cdot g_p$$

i =1,…,N$_{LOS}$ (LOS = line of sight)
p =1,…,N$_p$ (number of pixel in the reconstruction grid)
T: geometric matrix, g_p 2D emissivity evaluated in the p-reconstruction pixel

Ill-posed problem, T is not directly invertible.

We minimize the functional: $\phi = (1/2)\chi^2 + \lambda\Re$ to constrain the solution.

$\Re$ is the minimum of the Fisher Information which provides the smoothest solution, $I_F = \int \frac{\left(g'(x)\right)^2}{g(x)} dx$

λ is the parameter that regulates the smoothness of the solution.

The reconstruction algorithm minimizes I_F and targets the χ^2 to N$_{LOS}$ by iterations of λ.

We have defined: $\chi^2 = (\tilde{T} * g - \tilde{f}) * (\tilde{T} * g - \tilde{f})$, with $\tilde{T}_{ip} = T_{ip}/\sigma_i$ and $\tilde{f}_i = f_i/\sigma_i$, where σ_i is the standard deviation of f_i.

The number and distribution of the cameras is determined by a compromise between the quality of tomographic reconstruction and the cost, within the constraints set by the TCV port geometry.

A quantitative estimation of the quality of the reconstructed emissivity by assuming a given set of cameras (CS) used in the tomographic process is given by defining a **reconstruction variance (RV):**

$$RV_{CS}(R,O) = \frac{\sum_k \sum_n \left(\frac{R_{kn}}{\bar{R}} - \frac{O_{kn}}{\bar{O}} \right)^2}{\sqrt{\sum_k \sum_n (R_{kn}/\bar{R})^2 \sum_k \sum_n (O_{kn}/\bar{O})^2}}, \text{ where } \bar{F} = \left(\sum_k \sum_n F_{kn} \right) \Big/ N_p$$

which compares the original simulated emission (O) with the reconstructed one (R).

The **gain in the quality of the reconstruction** obtained by adding an additional camera is not a constant, the benefits being more significant when going from a 2 to a 3 camera setup and from 3 to 4 and becoming modest with each additional one. On the right-hand graph, the typical RV behavior for a particular *m=2* emission pattern is shown (see also the section below).

Tomographic validation

Best camera setup for N=2,3,4 tomographic camera system

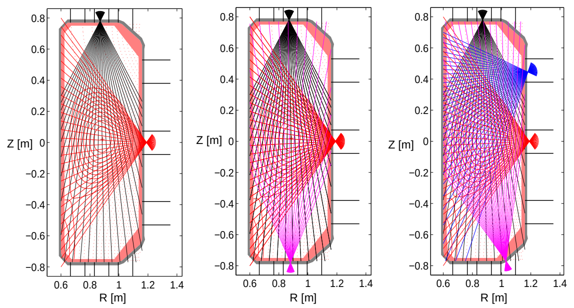

Cams: [C2,C5] Cams: [C2,C5,C8] Cams: [C2,C4,C5,C7]

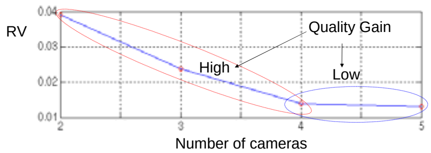

Tomographic Tests

Tomographic reconstructions of a *m* = 2 asymmetric emission pattern

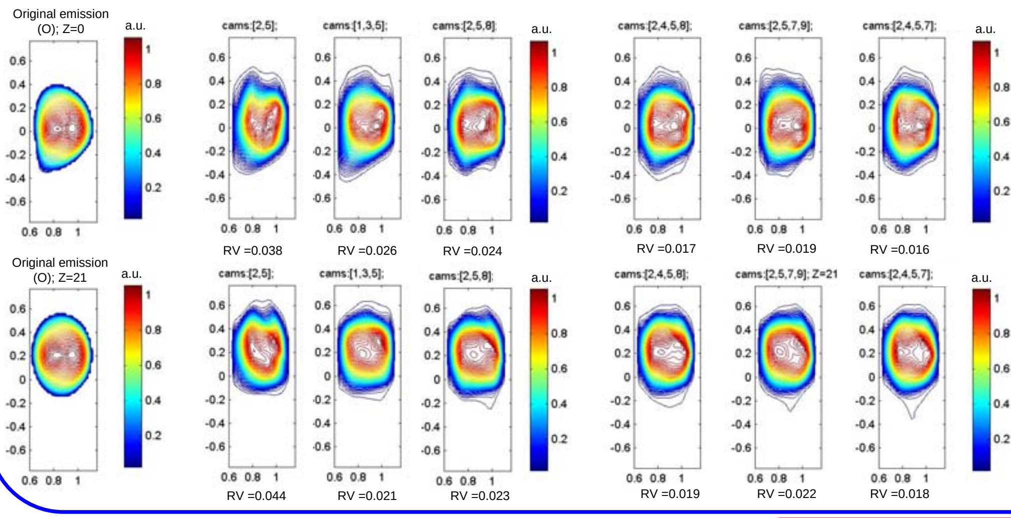

Tomographic reconstructions of a C3PO-LUKE-R5-X2[16] simulated bremsstrahlung emission.

- C3PO: ray-tracing code.
- LUKE: relativistic 3D bounce-averaged Fokker-Plank solver.
- R5-X2: bremsstrahlung calculator.

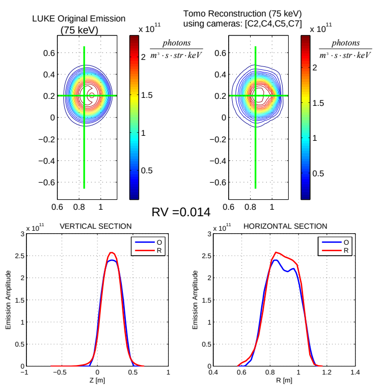

Peak position, relative intensity, and poloidal asymmetries have been recovered satisfactorily.

Conclusions:

The physics of heating and current drive and of MHD instabilities and their mitigation are all crucial to tokamak reactor operation and are tightly linked to the understanding of suprathermal electron generation and dynamics. To address these physics questions a novel design of a tomographic hard-X-ray spectrometer is being developed for the TCV tokamak. The design for different camera setups has been assisted by tomographic validation. The flexibility and compactness of the present design is expected to be readily adaptable to other fusion devices.

References:

[1] N.J. Fisch, Rev. Mod. Phys. **59**, 175 (1987).
[2] P.V. Savrukhin, Phys. Plasmas **9**, 3421 (2002).
[3] F. Hofmann et al, Plasma. Phys. Control. Fusion **36**, B277 (1994).
[4] Y. Peysson, F. Imbeaux, Rev. Sci. Instr. **70**, 3987 (1999).
[5] Y. Peysson, S. Coda, F. Imbeaux, Nucl. Inst. Meth. A **458**, 269 (2001).
[6] P. Blanchard, et al, Plasma. Phys. Control. Fusion **44**, 2231 (2002).
[7] S. Coda et al, Nucl. Fusion **43**, 1361 (2003).
[8] I. Klimanov et al, Plasma Phys. Control. Fusion **49**, L1 (2007).
[9] T.P. Goodman et al, Proc. 34th EPS Conf. on Control. Fusion and Plasma Phys., Warsaw, Poland, 2007 (P2.147).
[10] A. Sushkov et al, Rev. Sci. Instr. **79**, 023506 (2008).
[11] S. Alberti et al, Nucl. Fusion **42**, 42 (2002).
[12] S. Coda et al, Plasma. Phys. Control. Fusion **48**, B359 (2006).
[13] W. Soller, Phys. Rev. **24**, 158 (1924).
[14] B.R. Frieden, J. Mod. Opt. **35**, 1297 (1988).
[15] M. Anton et al, Plasma Phys. Control. Fusion **38**, 1849 (1996).
[16] J. Decker, Y. Peysson, DKE: "A fast numerical solver for the 3D drift kinetic equation", report EUR-CEA-FC-1736, Euratom-CEA (2004)